Modeling of Surfzone Bubbles Using a Multiphase VOF Model

Fengyan Shi[1], James T. Kirby[1], Merrick Haller[2], and Patricio Catalán[2]

We formulate a general multiphase model representing water-bubble mixture fluid and multi-component bubble populations. An enhanced 2-DV VOF model with a $k-\epsilon$ turbulence closure is used to model the mixture fluid phase. The bubble phase is governed by the advection-diffusion equations of the gas molar concentration and bubble intensity for groups of bubbles with different sizes. The initial bubble entrainment is formulated by connecting the flow shear stress at water-air interface and the bubble number intensity with a certain bubble size spectra as observed by Deane and Stokes (2002). The model is calibrated using the void fraction data measured in a plunging jet experiment (Hoque, 2002). The calibrated model is used to simulate regular wave transformation, breaking, and bubble generation and evolution processes over a barred bathymetry in the Long Wave Flume at Oregon State University. Model results are compared to measured data including both in-situ wave gages and video remote sensing.

INTRODUCTION

The ability to make optically-based observations in the surf-zone is strongly influenced by the presence of air bubbles, which are present due to the action of breaking waves. Wave breaking is instrumental in injecting large volumes of air into the water column. This air volume subsequently evolves into a distribution of bubble sizes that interact with the fluid turbulence and are advected by the organized flow. The bubble population in the surf-zone is intensified due to the greater intensity of breaking processes, leading to an increase in turbulence intensity and associated energy dissipation.

The processes of bubble entrainment and evolution are complex. According to previous studies based on field or laboratory experiments (e.g., Thorpe, 1982, Garrett, et al., 2000, Terrill, et al., 2001, Deane and Stokes, 2002), the lifetime of wave-generated bubbles can be categorized into two phases. The first phase is called the acoustic phase, during which bubbles are entrained and fragmented inside the breaking wave crest. The second phase happens after bubble creation processes cease and the newly formed bubbles evolve under the influence of turbulent diffusion, advection, buoyant degassing, and dissolution. Because this phase is acoustically quiescent it is called the quiescent phase. Some theoretical and observational studies suggest that, at the beginning of the quiescent phase, the size spectrum follows a certain power-law scaling with bubble radius. Bubbles larger and smaller than a so-called Hinze scale (Hinze, 1955) respectively vary as $(\text{radius})^{-10/3}$ and $(\text{radius})^{-3/2}$. Both slopes of the bubble size spectrum increase in time during the quiescent phase.

[1] Center for Applied Coastal Research, University of Delaware, Newark, DE 19716, USA
[2] School of Civil and Construction Engineering, Oregon State University, Corvallis, OR 97331, USA

Models for the distribution of bubble populations in the surfzone are rare, and, where they exist, are based on a simplified view of the circulation process of interest without involving detailed processes of bubble injection, interaction and evolution (for example, Vagle et al., 2001, 2005). The problem of bubble injection and initial distribution in the water column is happening on the time scale of the individual waves. A prediction of the distribution of bubbles over depth due to a breaking event depends on a good representation of the fluid velocity field at the wave-resolving time scale. The recent studies on 2-D (Gaeta et al., 2008) and 3-D (Liu and Lin, 2008) two-phase Navier-Stokes solvers showed the possibilities for directly predicting air packet entrainment and bubble evolution. They also indicated some difficulties in modeling air packet breakup, and small bubble entrainment and evolution processes because the requirement for higher resolution in both time and space can make a model computationally unaffordable.

In contrast with models that resolve individual bubbles, models based on volume averaged properties associated with bubble population are efficient. Carrica et al. (1998) reported a multiphase model in simulating bubbly two-phase flow around a surface ship. The bubble phase is modeled using the integrated Boltzmann transport equation for the bubble size distribution function (Guido-Lavalle et al., 1994) and the momentum equations for gaseous phase. The liquid phase is modeled using mass and momentum equations for liquid along with a turbulence closure. The air-liquid interactions are presented by drag, pressure, lift and buoyancy forces. The model accounts for intergroup transfer through bubble coalescence, dissolution and breakup. Buscaglia et al. (2002) developed a similar volume-averaged multiphase model without taking into account the momentum balance in the bubble phase. The exclusion of momentum equations for the bubble phase makes the model more efficient, especially in a simulation involving a number of bubble groups with different sizes.

In the present study, we formulate a general multiphase model representing a water-bubble mixed fluid and multi-component bubble populations following Buscaglia et al.'s (2002) approach. A 2-DV VOF model with a $k-\epsilon$ turbulence closure was modified to simulate the mixed fluid. The bubble phase containing a number of bubble groups with different sizes is modeled by solving advection-diffusion equations. The initial bubble entrainment is formulated by connecting the flow shear stress at the water-air interface and the bubble number intensity with certain bubble size spectra from prior measurements. The intergroup transfer during bubble evolution was evaluated based only on bubble size changes due to pressure without taking into account bubble breakup and coalescence. The model calibration was carried out using the void fraction data measured in a plunging jet experiment (Hoque, 2002). Next, the model was used to simulate regular wave transformation, breaking, and bubble generation and evolution processes over a barred bathymetry in the Long Wave Flume at Oregon State University.

FORMULATION

The multiphase model can be obtained by ensemble averaging the conservation equations for each phase in a multiphase flow, following Buscaglia et al. (2002).

Mixed Fluid Phase

The ensemble averaged equations include mass conservation and momentum equations for the mixture fluid phase:

$$\nabla \cdot \mathbf{u}_m = 0 \tag{1}$$

$$\frac{\partial \mathbf{u}_m}{\partial t} + \mathbf{u}_m \cdot \nabla \mathbf{u}_m + \frac{1}{\rho_0}\nabla P_m = \frac{1}{\rho_0}\nabla \cdot \left[\mu_t(\nabla \mathbf{u}_m + \nabla^T \mathbf{u}_m)\right] - \frac{\rho_m}{\rho_0} g\mathbf{k} \tag{2}$$

where $\mathbf{u}_m, P_m$ and ρ_m represent the mixture quantities of fluid velocity, pressure and density, respectively. ρ_0 is the so called reference density which has replaced ρ_m in all terms but the gravity term using the Boussinesq approximation. $\mathbf{k}$ is a vertical unit vector. μ_t is the eddy viscosity coefficient which is related to k and ϵ in the $k-\epsilon$ turbulence equations:

$$\mu_t = \rho_0 C_\mu \frac{k^2}{\epsilon} \tag{3}$$

where $C_\mu = 0.09$. The last term in (2) represents the buoyancy force which can be evaluated as

$$\frac{\rho_m}{\rho_0} g\mathbf{k} = (1 - \alpha_b) g\mathbf{k} \tag{4}$$

where α_b is the volume fraction of bubbles following the definitions in Drew and Passman (1998).

Bubble Phase

The equations for bubble phase include the equations of the gas molar concentration and bubble number intensity with different bubble sizes. Mass bin i of the bubble population are presently calculated using simple advection-diffusion equations given by

$$\frac{\partial C_b(i)}{\partial t} + \nabla \cdot (C_b(i)\mathbf{u}_g) = \mathcal{S}_c + \nabla \cdot (\mathcal{D}_g \nabla C_b(i)) \tag{5}$$

$$\frac{\partial N_b(i)}{\partial t} + \nabla \cdot (N_b(i)\mathbf{u}_g) = \mathcal{S}_n + \nabla \cdot (\mathcal{D}_g \nabla N_b(i)) \tag{6}$$

where $C_b(i)$ and $N_b(i)$ represent, respectively, the gas molar concentration and bubble number per unit volume for bubble size i. $\mathbf{u_g}$ is the bubble advection velocity which can be calculated by

$$\mathbf{u}_g = \mathbf{u}_m + w_s(r_b)\mathbf{k} \tag{7}$$

in which $w_s(r_b)$ is the bubble-slip velocity, assumed only depending on the bubble radius based on Clift et al. (1978):

$$w_s = \begin{cases} 4474 \text{ m/s} \times r_b^{1.357} & \text{if } 0 \leq r_b \leq 7 \times 10^{-4} m \\ 0.23 \text{ m/s} & \text{if } 7 \times 10^{-4} < r_b \leq 5.1 \times 10^{-3} m \\ 4.202 \text{ m/s} \times r_b^{0.547} & \text{if } r_b > 5.1 \times 10^{-3} m \end{cases} \tag{8}$$

$\mathcal{S}_c$ and $\mathcal{S}_n$ are source/sink terms associated with inter-group adjustment of bubble quantity between different component i caused by bubble size changes due to pressure change, bubble breakup and coalescence. $\mathcal{D}_g$ is the dispersion coefficient associated with the turbulence and bubble-bubble interaction. In the isotropic model proposed by Carrica et al. (1998),

$$\mathcal{D}_g = \frac{\mu_t}{\rho_0 S_g} \tag{9}$$

where S_g is the Schmidt number for gas. The gas volume fractions used in (4) can be calculated using

$$\alpha_b = \frac{\mathcal{R} T_g \sum_i C_b(i)}{P_g} \tag{10}$$

where $\mathcal{R}$ is the universal gas constant, i.e., 8.314 J/mol K. T_g is the absolute gas temperature, P_g is gas pressure, assumed equivalent to P_m. The bubble radius can be calculated using

$$r_b(i) = \left(\frac{3\nu_b(i)}{4\pi} \right)^{1/3} \tag{11}$$

where $\nu_b(i)$ is the bubble volume of component i which can be obtained by

$$\nu_b(i) = \frac{C_b(i) \mathcal{R} T_g}{P_g N_b(i)} \tag{12}$$

NUMERICAL IMPLEMENTATION AND CALIBRATION

We used the 2-D VOF model, RIPPLE (Kothe et al., 1991), as the basic framework for the computational code. The VOF model has been enhanced with several different turbulence closure models such as $k-\epsilon$ model (Lin and Liu, 1998) and multi-scale LES model (Zhao et al., 2004, Shi et al., 2004). The buoyancy force was added in the momentum equation (2) according to (4) in which the void fraction α_b may be evaluated using (10).

Bubbles are separated into a number of groups with different sizes by equal splitting in the logarithm of bubble radius. The gas molar concentration and bubble number intensity for each group are governed by (5) and (6). The intergroup transfer is predicted according to bubble size changes based on (11) and (12). The governing equations (5) and (6) were implemented using the standard numerical schemes for advection-diffusion equations which exist in the VOF model code.

The initial bubble entrainment is formulated by connecting the production of flow shear stress at water-air interface and the bubble number intensity with certain bubble size spectra observed by Deane and Stokes (2002) and others. The increment of initial bubble number intensity can be written as

$$dN(i) = a_b \nu_T \left(\nabla \mathbf{u}_m + \nabla^T \mathbf{u}_m \right) r(i)^{\alpha} dr dt \tag{13}$$

where α represents the slope of initial bubble size distribution, particularly in this study, $\alpha = -3/2$ if $r_b \leq 1$ mm and $\alpha = -10/3$ if $r_b > 1$ mm. a_b is a constant. For given $r_b(i)$, $N_b(i)$ and P_g, the initial molar concentration associated with bubble entrainment is calculated using (11) and (12). During the bubble evolution process, (12) is used again to get the bubble size change due to pressure changes. Temperature T_g is kept constant during the whole process. The constant a_b in (13) is determined using the void fraction data measured in a plunging jet experiment (Hoque, 2002).

APPLICATION TO WAVE EXPERIMENT IN A LONG WAVE FLUME

The calibrated model is used to simulate regular wave transformation, breaking, and bubble generation and evolution processes over a barred bathymetry in a large scale laboratory experiment. Figure 4 shows the experimental layout for LWF, including bathymetric profile and wave gage locations.

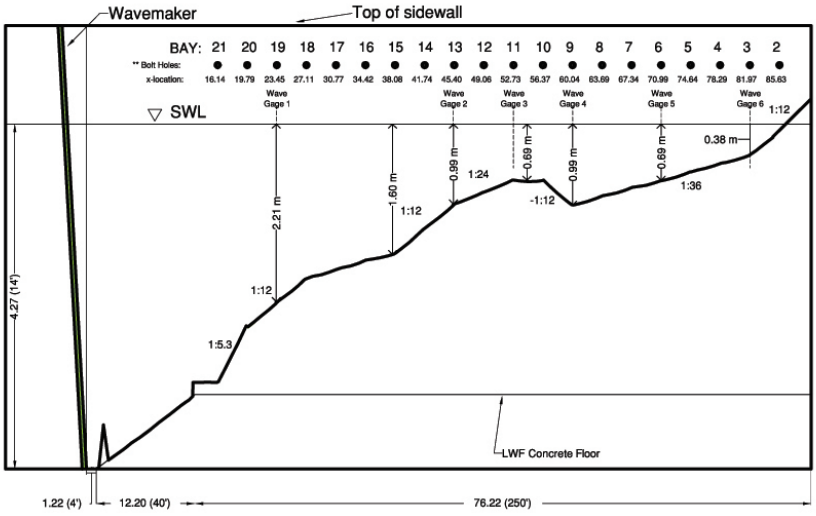

Figure 1. Experimental layout for the Large Wave Flume, including bathymetric profile and wave gauge locations.

With the model we carried out simulations of a monochromatic wave case with a period of 5 s and compared numerical results with the available data from the experiment. Figure 2 and 3 show model/data comparisons of surface elevation at Gauge 1 - 6. Good agreements between the numerical results and the data were found at all the six gauge locations.

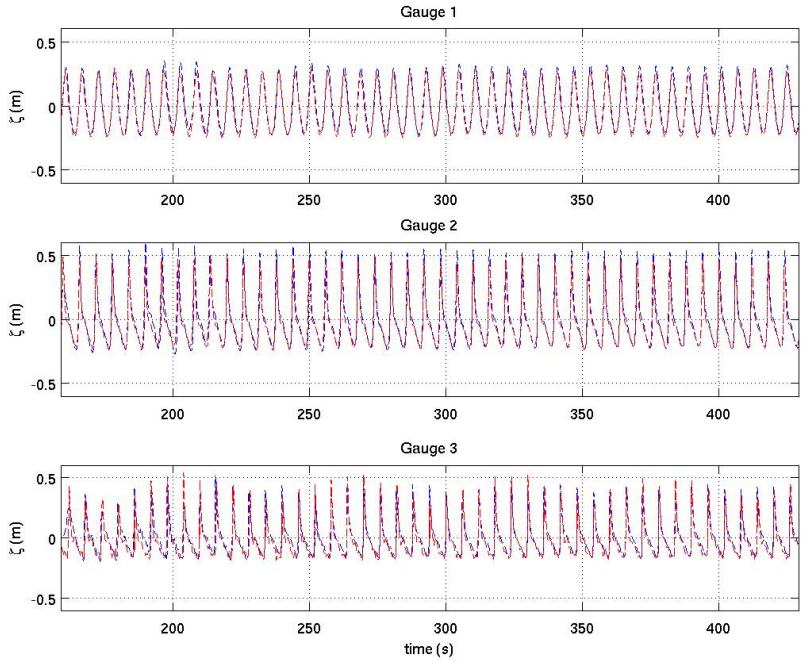

Figure 2. Comparison of surface elevation between modeled results (solid lines) and measured data (dashed lines) at Gauge 1-3.

Figures 4 - 6 demonstrate time evolution of the breaking wave and void fraction (contours) calculated from the model. The maximum void fraction can be found at the breaking wave crest and the large values basically remain close to the water surface. The void fraction distributions may also indicate that there is an overall spatial patchiness in bubble clouds when measured in terms of distance behind the wave crest. The patchiness can be seen in Figure 7 which shows the foam and bubble signature on the water surface following the passage of breaking wave crests, as sensed by video systems during the experiment. The time stack of the cross-shore distribution of modeled surface void fraction is shown in Figure 8. The figure indicates the consistency between the foam signature and the modeled void fraction.

As observed in field experiments (Deane and Stokes, 2002) bubble size

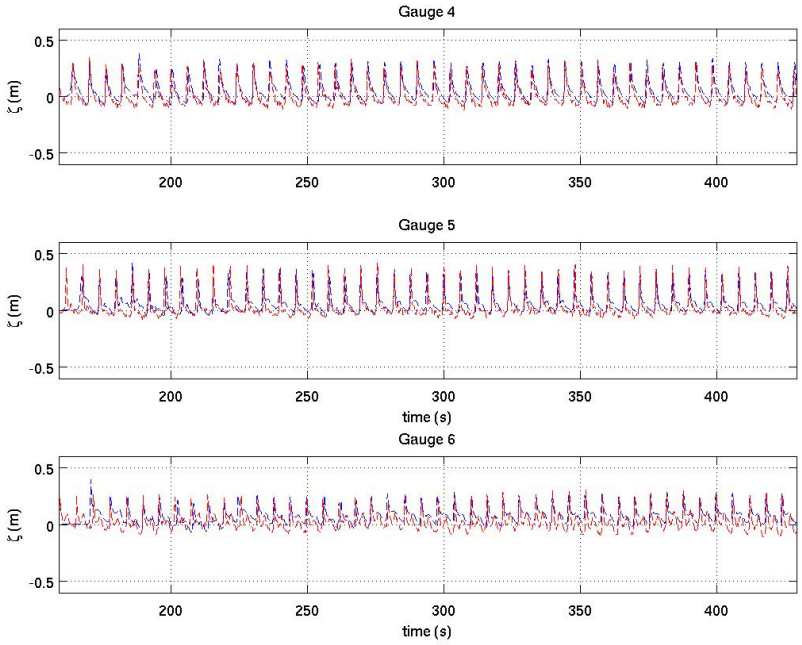

Figure 3. Comparison of surface elevation between modeled results (solid lines) and measured data (dashed lines) at Gauge 4-6.

spectrum changes in time during the evolution of bubble populations. The evolution of bubble size spectrum is demonstrated in Figure 9 and 10 which show the bubble number intensity versus the bubble radius at several vertical levels at $t = 143s$ and $t = 147s$, respectively. The figures show that the slopes of size distribution increase in time for an individual breaker. Although these numerical results are qualitatively consistent with the field observations, it is noticed that the changes in the distribution slopes are less obvious than the measurements (Deane and Stokes, 2002). It may suggest that the mechanism of further bubble breakup is important and should be taken into account in the model.

We also made comparisons between the previous model without a bubble phase and the present model with a bubble phase. The comparisons indicated that bubbles have significant effects on wave flow patterns, surface elevations and turbulence distributions. Here we do not make further discussions because the model, at this stage, only takes into account buoyancy effects in the mixed fluid phase.

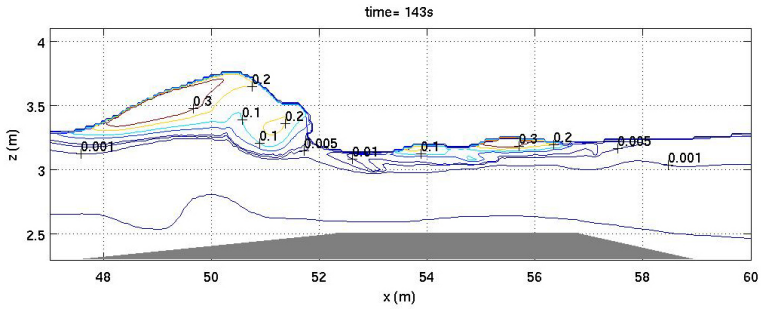

Figure 4. Modeled void fraction after wave breaking at t = 143 s.

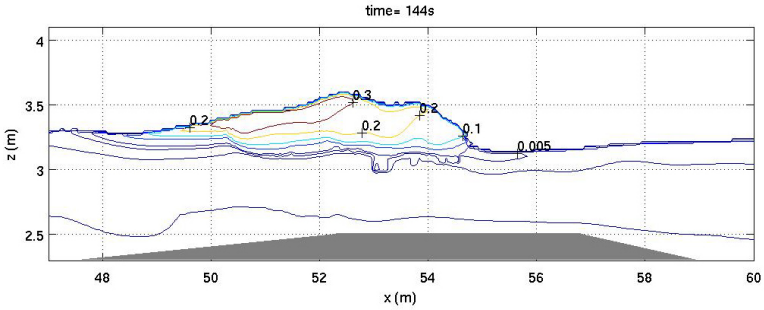

Figure 5. Modeled void fraction after wave breaking at t = 144 s.

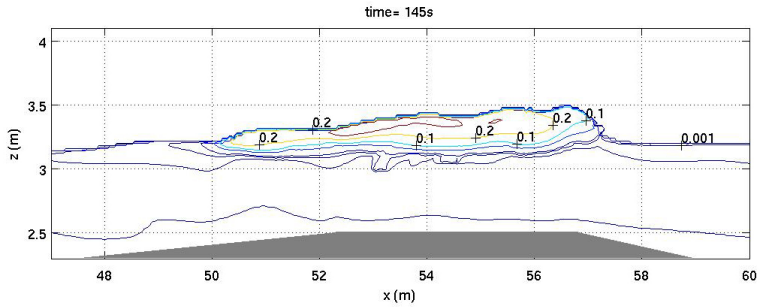

Figure 6. Modeled void fraction after wave breaking at t = 145 s.

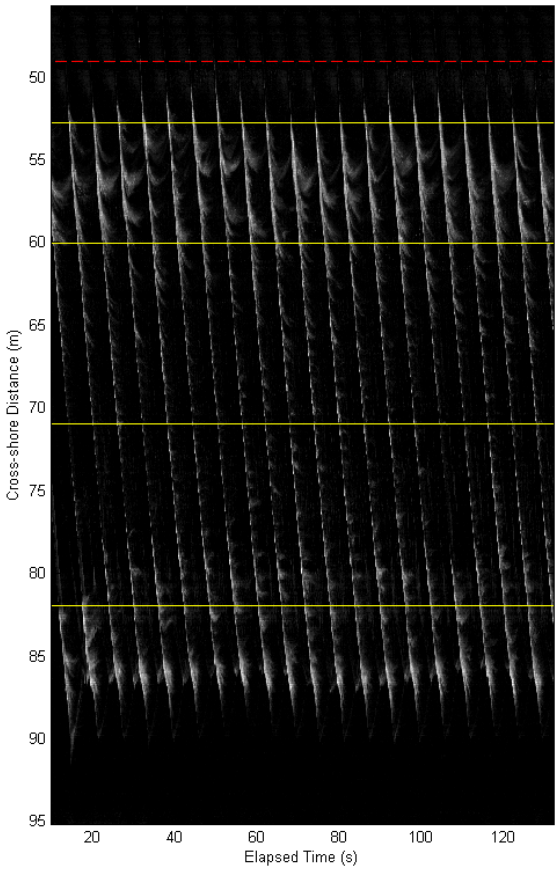

Figure 7. Time stack of bubble foam signature on the water surface sensed by video systems. Horizontal lines denote wave gage locations.

CONCLUSION

A 2DV multiphase model was developed to simulate water and multi-component bubble populations. The governing equations include mass conservation and momentum equations for a mixed fluid phase, the gas molar concentration and bubble number intensity equations for groups of bubbles with different sizes. The initial bubble entrainment was formulated by connecting the production of flow shear stress at water-air interface and bubble number intensity with certain bubble size spectra observed by Deane and Stokes (2002). The model

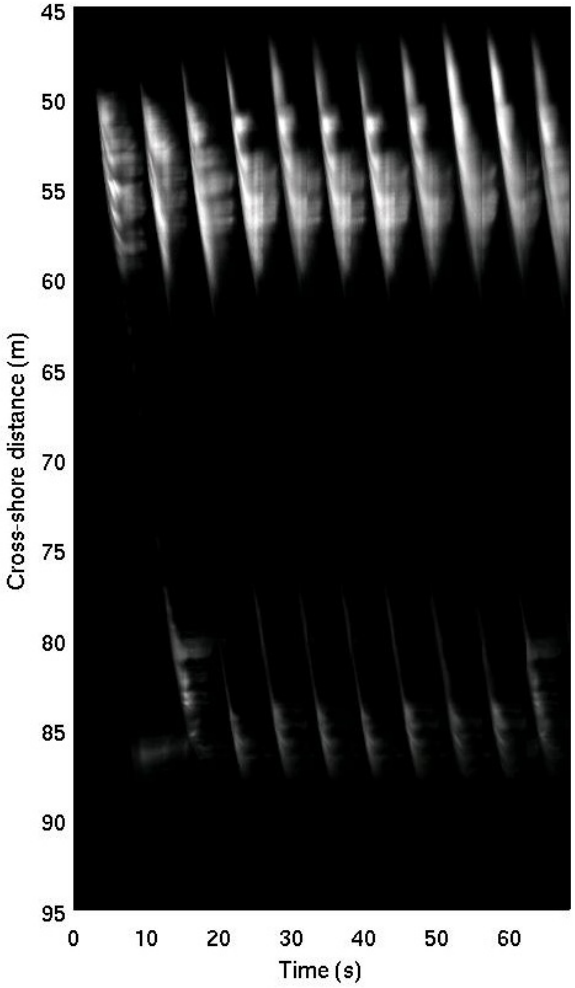

Figure 8. Time stack of modeled void fraction on the water surface.

calibration was carried out using the void fraction data measured in a plunging jet experiment (Hoque, 2002). The model was applied to simulations of wave transformation, breaking, and bubble generation and evolution processes over a barred bathymetry in the Long Wave Flume at Oregon State University. The surface elevations predicted in the model agree well with the measured data at several measurement locations. The modeled void fractions on the water surface were compared to the bubble foam signatures sensed by video systems during the laboratory experiments and a qualitative consistency was found.

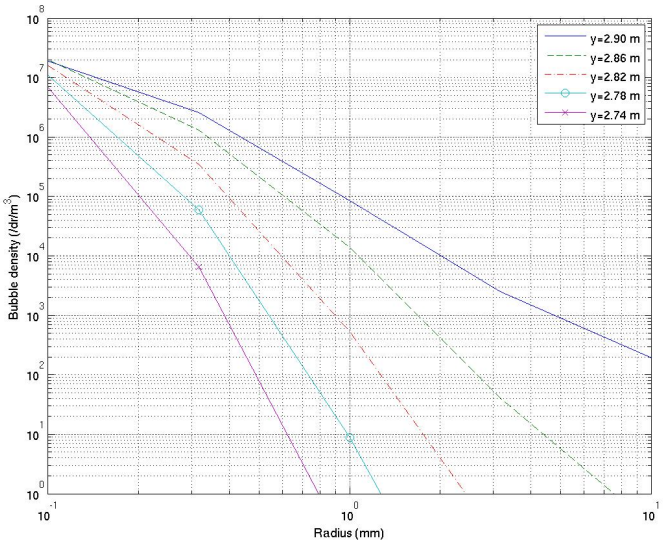

Figure 9. Bubble size distribution at $x = 55m$ and $t = 143s$

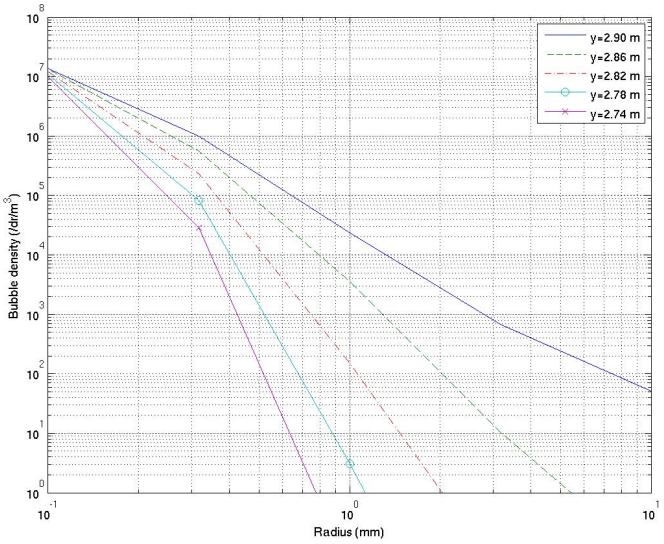

Figure 10. Bubble size distribution at $x = 55m$ and $t = 147s$

The model may not predict detailed bubble entrainment and fragmentation processes in the acoustic phase. The interactions between the liquid phase and bubble phase, turbulence and bubbles are not very well addressed in the model. A more complete development will be reported on in the near future, in conjunction with more comprehensive implementations of wave coalescence, dissolution, further breakup and turbulence and bubble interaction.

ACKNOWLEDGMENTS

This study was supported by Office of Naval Research, Coastal Geoscience Program under grant N00014-07-1-0582. M. Haller and P. Catalán were supported under grant number N00014-02-1-0147.

REFERENCES

Buscaglia G. C., Bombardelli F. A., and Garcia M H., 2002, Numerical modeling of large-scale bubble plumes accounting for mass transfer effects, *International Journal of Multiphase Flow*, 28, 1763-1785

Carrica P. M., Bonetto F., Drew D. A., Lahey R. T. Jr, 1998, The interaction of background ocean air bubbles with a surface ship, *Int. J. Numer. Meth. Fluids*, 28, 571-600.

Clift, R., Grace, J., Weber, M., 1978, *Bubbles, Drops and Particles*, Academic Press.

Deane, G. B. and Stokes, M. D., 2002, Scale dependence of bubble creation mechanisms in breaking waves, *Nature* 418, pp. 839844.

Drew D and Passman S., 1998, *Theory of multicomponent fluids*, Springer.

Gaeta, M. G., Lamberti, A., and Liu, P. F.-L., 2008, Two-phase breaking wave numerical model for incompressible fluids: Air influence and applications, *Proceeding of the 31st International Conference*, Hamburg.

Garrett C., Li M., and Farmer D., 2000, The connection between bubble size spectra and energy dissipation rates in the upper ocean, *Journal of Physical Oceanography*, 30, 2163-2171.

Guido-Lavalle, G., Carrica, P., Clausse, A., and Qazi, M. K., 2004, A bubble number density constitutive equation, *Nuclear Engineering and Design*, 152, 1-3, 213-224.

Hinze, J. O., 1955, Fundamentals of the hydrodynamic mechanism of splitting in dispersion processes, *Amer. Inst. Chem. Eng. J.*, 1, 289295.

Hoque, A, 2002. Air bubble entrainment by breaking waves and associated energy dissipation, PhD Thesis, Tokohashi University of Technology.

Kothe, D. B., Mjolsness, R. C. and Torrey, M. D., 1991, RIPPLE: a computer program for incompressible flows with free surfaces, Los Alamos National Laboratory, Report LA 12007 MS.

Lin P. and Liu P. L.-F, 1998, Turbulence transport, vorticity dynamics, and solute mixing under plunging breaking waves in surfzone, *J. Geophys. Res.*, 103, 15677-15694.

Liu, D. and Lin, P., 2008, A numerical study of three-dimensional liquid sloshing in tanks, *Journal of Computational Physics*, 227(8), 3921-3939.

Shi F., Zhao Q., Kirby J. T., Lee, D. S., and Seo S. N. 2004, Modeling wave interaction with complex coastal structures using an enhanced VOF model, *Proceedings of the 29th International Conference*, Vol. 1, 581-593.

Terrill E. J., Melville W. K., and Stramski D., 2001, Bubble entrainment by breaking waves and their influence on optical scattering in the upper ocean, *J. Geophys. Res.*, 106, C8, 16,815-16,823.

Thorpe S. A., 1982, On the clouds of bubbles formed by breaking wind-waves in deep water, and their role in air-sea gas transfer, *Phil. Trans. Roy. Soc. London A*, 304, 155-210.

Vagle S., Farmer D. M. and Deane G. B., 2001, Bubble transport in rip currents, *J. Geophs. Res.*, 106, C6, 11,677 - 11,689.

Vagle S., Chandler P. and Farmer D. M., 2005, On the dense bubble clouds and near bottom turbulence in the surfzone, *J. Geophys. Res.*, 110, C09018, doi:10.1029/2004JC002603.

Zhao, Q., Armfield, S., and Tanimoto, K., 2004, Numerical simulation of breaking waves by a mult-scale turbulence model, *Coastal Engineering*, 51, 53-80.

KEYWORDS – ICCE 2008

PAPER TITLE: Modeling of Surfzone Bubbles Using a Multiphase VOF Model
Authors: Fengyan Shi, James T. Kirby, Merrick Haller, and Patricio Catalán
Abstract number 315

Air bubble
Multiphase model
Navier-Stakes solver
VOF model
Surfzone